(1985) *Biochemistry 24*, 6639–6645.

Potter, J. D., Strang-Brown, P., Walker, P. L., & Iida, S. (1983) *Methods Enzymol. 102*, 135–143.

Rhee, M.-J., Sudnick, D. R., Arkle, V. K., & Horrocks, W. DeW., Jr. (1981) *Biochemistry 20*, 3328–3334.

Stein, G., & Würzberg, E. (1975) *J. Chem. Phys. 62*, 208–213.

Tingey, J. M. (1987) Ph.D. Thesis, The Pennsylvania State University, University Park, PA.

Tsai, M.-D., Drakenberg, T., Thulin, E., & Forsén, S. (1987)

Biochemistry 26, 3635–3643.

Valentini, M. A., & Wright, J. C. (1985) *Anal. Biochem. 150*, 47–57.

Wallace, R. W., Tallant, E. A., Dockter, M. E., & Cheung, W. Y. (1982) *J. Biol. Chem. 257*, 1845–1854.

Wang, C.-L. A., Aquaron, R. R., Leavis, P. C., & Gergely, J. (1982) *Eur. J. Biochem. 124*, 7–12.

Wang, C.-L. A., Leavis, P. C., & Gergely, J. (1984) *Biochemistry 23*, 6410–6415.

Fluorescence Anisotropy Decay Demonstrates Calcium-Dependent Shape Changes in Photo-Cross-Linked Calmodulin[†]

Enoch W. Small* and Sonia R. Anderson

Department of Biochemistry and Biophysics, Oregon State University, Corvallis, Oregon 97331

Received June 2, 1987; Revised Manuscript Received August 18, 1987

ABSTRACT: We report dynamic fluorescence anisotropy measurements on the purified dityrosine derivative of calmodulin which was generated during UV irradiation of Ca^{2+}-containing solutions of bovine brain calmodulin [Malencik, D. A., & Anderson, S. R. (1987) *Biochemistry 26*, 695]. Measurements were made by using a high repetition rate picosecond laser source combined with a microchannel plate photomultiplier. This permits the collection of very low noise anisotropy curves with essentially no convolution artifact. Measured anisotropies at high calcium concentrations are monoexponential, and at 20 °C, we recover a correlation time of 9.9 ns. When the temperature is varied from 4.8 to 31.8 °C, the recovered correlation time is proportional to the viscosity and inversely proportional to the absolute temperature, behavior expected for the rotational diffusion of a macromolecule whose conformation is independent of the temperature. The correlation time is compared to the theory describing the rotational diffusion of a dumbbell. At high calcium concentrations, the cross-linked calmodulin is elongated and has a length equal or nearly equal to that predicted by X-ray crystallographic results. In the absence of calcium, the molecule becomes highly compact and exhibits significant segmental motion. Intermediate calcium ion concentrations result in an intermediate degree of elongation and segmental motion. A small increase in the measured rotational correlation time of calmodulin upon the binding of melittin and mastoparan indicates that these peptides cause no major changes in the elongation of the molecule. When the cross-linked calmodulin is bound to troponin I, the complex rotates as a unit with a single rotational correlation time of 22 ns.

Calmodulin is a small acidic protein with a molecular weight of 16 700. In eukaryotic cells, it is the primary mediator of calcium control for a number of metabolic processes. For example, it binds and activates cyclic nucleotide phosphodiesterase (Cheung, 1967), adenylate cyclase (Cheung et al., 1975; Brostrom et al., 1975), and myosin light chain kinase [cf. Perry et al. (1984)]. It also interacts with a number of basic small peptides which compete with the enzymes in the in vitro binding of calmodulin [cf. Anderson and Malencik (1986, 1987)]. Since these associations are strongly calcium dependent, the binding of calcium by calmodulin apparently stabilizes one or more conformations which are conducive to the binding of specific proteins and peptides.

X-ray crystallographic studies of the calcium–calmodulin complex performed at 3.0-Å resolution have revealed a dumbbell-shaped molecule containing two lobes connected by an eight-turn α-helix (Babu et al., 1985). The total length of the molecule is about 65 Å. Each lobe has the approximate dimensions of 25 × 20 × 20 Å and binds two calcium ions through helix–loop–helix domains similar to those found in other calcium-binding proteins. Although the three-dimensional structure of calcium-free calmodulin is still unknown, a number of physical methods have demonstrated conformational changes in calmodulin upon the binding of calcium. These include circular dichroism (Klee, 1977; Wolff et al., 1977; Crouch & Klee, 1980; Hennessey et al., 1987), nuclear magnetic resonance [Seamon, 1980; cf. review by Forsén et al. (1986)], fluorescence (Kilhoffer et al., 1981; Lambooy et al., 1982), and ultraviolet difference spectroscopy (Klee, 1977; Crouch & Klee, 1980). The results obtained with these techniques deal with the microscopic environments of particular chromophores rather than with the overall hydrodynamic properties of the calmodulin molecule. Consequently, they give incomplete information on many of the distinctive structural perturbations initiated by Ca^{2+} binding. For example, circular dichroism—which examines the secondary structure of proteins—reveals little difference between calmodulin folded in potassium chloride in the absence of calcium and calcium-saturated calmodulin (Hennessey et al., 1987). The rotational diffusion studies reported here, on the other hand, are highly

sensitive to the overall tertiary structue of the calmodulin.

Vertebrate calmodulin contains two tyrosine residues at positions 99 and 138, located in the third and fourth calcium-binding domains, respectively. The tyrosines are close together in the three-dimensional structure, with the loop regions of calcium-binding sites III and IV connected by a hydrogen bond between Ile-100 and Val-136. Tyr-99 faces into the third calcium-binding site and is partially accessible to solvent while Tyr-138 points away from the fourth calcium-binding loop, into a hydrophobic pocket, making contact with Phe-89 and Phe-141 (Babu et al., 1985). Irradiation of the calcium–calmodulin complex at 280 nm results in the coupling of Tyr-99 and Tyr-138 (Malencik & Anderson, 1987). The singly ionized dityrosine (2,2'-biphenol derivative) chromophore of calmodulin is characterized by an absorption maximum near 320 nm and an emission maximum at 400 nm, wavelengths which are well separated from the excitation and emission maxima of tyrosine. These properties were utilized in steady-state fluorescence intensity and anisotropy measurements, which demonstrated that the cross-linked calmodulin molecule associates both with calcium and with smooth muscle myosin light chain kinase, but at a diminished level of effectiveness.

This report summarizes the results of anisotropy decay measurements on the dityrosine fluorescence of cross-linked calmodulin. The rigid attachment of the probe to the protein makes it especially suitable for these studies. The results are interpreted by using dumbbell and ellipsoid models for rotational diffusion. We also examine the binding of the cross-linked calmodulin to troponin I and to the peptides melittin and mastoparan.

MATERIALS AND METHODS

Materials. The preparation, purification, and characterization of the cross-linked calmodulin have been described in detail by Malencik and Anderson (1987). Protein concentrations were 1.0–2.0 μM in specific experiments in 50 mM 3-(N-morpholino)propanesulfonic acid (MOPS) buffer at pH 7.5. Other conditions are specified in the text. A sample of dityrosine was prepared in an enzyme-catalyzed reaction and subsequently purified, as described by Amado et al. (1984).

Troponin I was prepared from rabbit skeletal muscle following the procedure of Potter (1982). Mastoparan was purchased from Peninsula Laboratories and melittin (85% purity) from Sigma Chemical Co.

Instrumentation. The monophoton fluorescence decay instrument used in these studies was recently described in the literature (Small et al., 1984), but a number of changes have been made since that time which affect the quality of the results presented here. The changes include the addition of a Hamamatsu R1564U triple microchannel plate photomultiplier, new timing electronics, and a new method of energy windowing to reject multiple photon events.

The electronic modules are briefly summarized in the block diagram in Figure 1. In this current system, the output of the photomultiplier is fed to a Hewlett Packard Model 8774E power amplifier (recommended by Hamamatsu). Since this amplifier has an AC-coupled input, it is necessary to place either an attenuator or a simple terminator on the input. We have found a 100-Ω terminator to be satisfactory. The output of the amplifier is split with an Avtech model AVX-SP-4 splitter. The resulting negative pulse is used for timing, and the positive pulse is used for energy windowing.

The timing pulse is fed to a Phillips Scientific Model 6915 constant fraction timing discriminator (CFTD). The output of the discriminator is used to start an Ortec Model 467 time
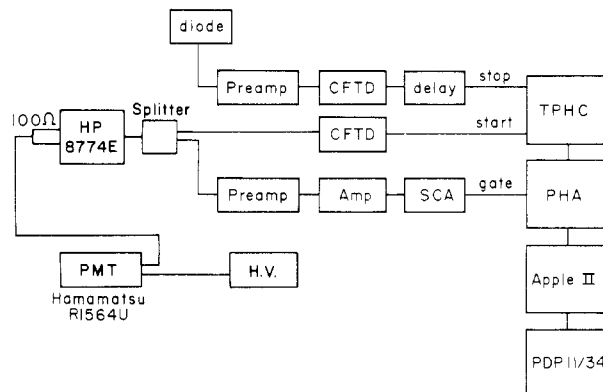

FIGURE 1: Block diagram of the electronics of the fluorescence decay instrument.

to pulse height converter (TPHC). The output of a Spectra-Physics Model 403B high-speed photodiode is amplified by a Phillips Scientific Model 6954 pulse amplifier and the timing pulse generated in a 6915 timing discriminator. The discriminator output must be delayed before use by the time to pulse height converter.

For energy windowing, the positive output of the splitter is amplified in an Ortec Model 474 timing filter amplifier. By use of the highest integration setting of 500 ns, this unit functions as a preamplifier and is capable of producing the stretched pulses needed for integrating multiple photon events. Integration is performed by an Ortec 485 amplifier. The 485 output is then windowed through an Ortec 420 single-channel analyzer, and the resulting pulse is delayed and broadened in an Ortec 416 gate and delay generator. This pulse is then used to gate the pulse height analyzer (PHA) to record only single photon events.

For the analyses of fluorescence anisotropies reported here, it is important for the measured excitation to drop rapidly to negligible values. An example of a measured excitation obtained with a dilute Ludox scatter sample can be seen in Figure 2. At low nanoseconds per channel, we measure a half-width of about 80 ps using the above system. It is obviously difficult to specify a half-width at the higher 0.0464 ns/channel used in these studies. Of more interest for these measurements, the widths at 1/10, 1/100, 1/1000, and 1/10000 of the maximum value are 0.464, 1.02, 209, and 2.78 ns, respectively.

At 0.0464 ns/channel, more than half of the integrated intensity occurs within three channels, with one channel clearly dominating. We found that the timing of the instrument is extremely stable and over 8 h of measurement the peak channel did not change. The data collection rate was manually maintained near 20 kHz for all samples in order to maximally utilize the collection capabilities of the instrument and to minimize artifacts due to changes in photomultiplier gain resulting from different count rates. At the 20-kHz counting rate, 2.4×10^7 monophoton counts of data require 20 min of collection.

The Spectra-Physics synchronously pumped dye laser system was used as a light source for the decay fluorometer. The dye laser is cavity-dumped at 800 kHz and the output frequency-doubled to the UV. Because we frequently require 280-nm light for exciting the tyrosine fluorescence of proteins, we use the dye rhodamine 575 obtained from Exciton Chemical Corp. (Libertini & Small, 1987). A 310-nm excitation wavelength was used for all decay experiments. This wavelength is near the peak of the dityrosine absorbance but outside the absorbance of tyrosine in unreacted calmodulin which may be present in the sample, or tryptophan in melittin.

Sensitivity Correction. With such low noise, we found the accuracy of our analyses to depend largely on the accuracy of the sensitivity correction used for normalizing the intensities of the parallel and perpendicular components of the fluorescence. The need for an accurate sensitivity correction is a well-recognized problem in measurements of anisotropy decay (Badea & Brand, 1979). Anisotropy, r, was calculated from the parallel and perpendicular components of the fluorescence, $F_{\parallel}$ and $F_{\perp}$ from

$$r(t) = \frac{F_{\parallel} + SF_{\perp}}{F_{\parallel} + 2SF_{\perp}} \qquad (1)$$

Thus, we are assuming a δ function excitation. The total sensitivity correction, S, was found as the product of three ratios:

$$S = \frac{\text{sum}_{\parallel}}{\text{sum}_{\perp}} \frac{I_{v,h}}{I_{v,v}} \frac{I_{h,v}}{I_{h,h}} \qquad (2)$$

where $\text{sum}_{\parallel}$ and $\text{sum}_{\perp}$ are the integrated intensities of $F_{\parallel}$ and $F_{\perp}$, respectively, from their initial rise out to 39 ns. Intensity values correspond to instrumental counting rates for vertical (v) or horizontal (h) orientations of the polarizers, where the first subscript defines the orientation of the incident polarizer and the second subscript defines that of the emission polarizer. These intensities were measured at low counting rates below 5 kHz where the response of the instrument is linear. Normally, the ratio of intensities using horizontally polarized excitation is called the sensitivity correction. In the experiments presented here, we found this ratio to be nearly equal to 1, ranging from 1.01 to 1.06. It remained constant throughout a day's measurements.

Intensity decays were measured without a sensitivity correction in the standard manner with vertical incident polarization and with the emission polarizer at the "magic angle" of 54.74° from the vertical.

Data Analysis. Results were analyzed by using the method of moments with λ invariance and moment index displacement, MD (Isenberg & Small, 1982; Small et al., 1984). We make use of the Cheng–Eisenfeld filter, a method of fixing the lifetime of a fluorescent component and recovering its amplitude from the analysis (Cheng & Eisenfeld, 1979). We have shown this approach to be successful in determining an amount of a trace component in the fluorescence and removing its effect on the resolution of remaining decays (Libertini & Small, 1982). We have also developed a method using the Cheng–Eisenfeld moment filter for recovering underlying distributions of lifetimes in nonexponential decays. Anisotropy decays were analyzed by using new method of moments programs for the analysis of nonconvoluted functions. These programs incorporate λ invariance, MD, and a global analysis. Details of these programs will be published elsewhere.

Although not an integral part of the method of moments analysis, to examine the experimental fit to the data reduced χ^2 was calculated from

$$\chi^2 = \frac{1}{N - n} \sum_{i=1}^{N} \frac{(r_{i,m} - r_{i,c})^2}{\text{Var}(r_i)} \qquad (3)$$

where N is the number of channels of data, n is the number of decay parameters (amplitudes and lifetimes), and $r_{i,m}$ and $r_{i,c}$ are the measured and calculated values of the anisotropy at channel i, respectively. The variance is given by

$$\text{Var}(r_i) = \frac{9S^2 F_{i,\parallel}(F_{i,\parallel} + F_{i,\perp})}{(F_{i,\parallel} + 2SF_{i,\perp})^4} \qquad (4)$$
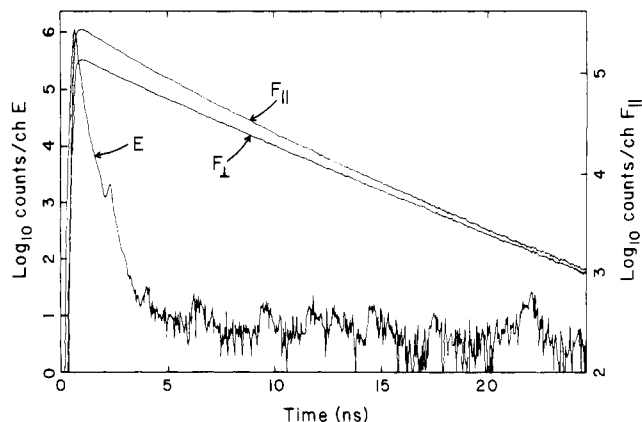
FIGURE 2: Logarithmic plots of the measured excitation, E, and the polarized fluorescence intensity decays, $F_{\parallel}$ and $F_{\perp}$, for 1 μM cross-linked calmodulin in 20 mM calcium acetate and 50 mM MOPS at pH 7.5 and 20.0 °C. Fluorescence excitation was at 310 nm using a picosecond laser system, and emission was measured through a Corning O-52 cutoff filter. Data were collected at 0.0464 ns/channel, and about 650 channels are shown.

where $F_{i,\parallel}$ and $F_{i,\perp}$ are the parallel and perpendicular components of the fluorescence at channel i, respectively.

These experiments have been designed to study the relatively long relaxation times of the protein. Due to the fast instrument response time, we assume that the fluorescence is a δ function response and calculate the anisotropy directly. We set time = 0.0 at the peak of the measured excitation and begin our data analysis 1.3 ns later, at the point at which the measured excitation has dropped below 0.2% of its maximum value. While these are rather arbitrary choices, varying these positions by a few hundred picoseconds either way has no significant effect on the results reported here. We take this as an indication that convolution artifacts are not affecting recovered parameters. Although the analysis begins at the point indicated on the plot, amplitudes are extrapolated back to the position of zero time.

RESULTS

Anisotropy Decays as a Function of Calcium Ion Concentration. Polarized fluorescence decays were measured for cross-linked calmodulin at five calcium concentrations from 0.0 [with 15 μM ethylenediaminetetraacetic acid (EDTA)] to 20 mM at 20 °C. The range of calcium concentrations is based on steady-state measurements, which showed that Ca^{2+} binding by the derivative occurs in two stages—with saturation approached at concentrations of 10–20 mM (Malencik & Anderson, 1987). Sample decay data measured at the high calcium concentration are shown in Figure 2. Three curves are plotted—the measured excitation, E, the fluorescence measured through a vertical polarizer, $F_{\parallel}$, and the horizontal component, $F_{\perp}$. Each fluorescence decay curve contains approximately 2.4 × 10^7 counts of data. Relatively large numbers of counts are necessary in order to extend the useful range of the anisotropy data beyond several lifetimes of the fluorescence. Under the conditions used, the measured excitation is very narrow (see Materials and Methods for more information about the shape of the instrument response). Because of this fast instrument response, we can use these data to calculate the anisotropy directly without deconvolution.

Anisotropy decays calculated according to eq 1 for the 0.0 and 20 mM calcium concentrations are shown in Figure 3A. Visually, the anisotropy of the cross-linked calmodulin at 20 mM calcium appears monoexponential for at least 24 ns of decay. As we will show below, this is approximately 6 times the average lifetime of the fluorescence. There is also very

Table I: Analyses of Anisotropy Decays of Cross-Linked Calmodulin at Various Calcium and KCl Concentrations[a]

[Ca²⁺]	[KCl] (mM)	unfiltered					filtered[b]			
		β_1	ϕ_1	β_2	ϕ_2	$\beta_1 + \beta_2$	β_1	ϕ_1	β_2	ϕ_2
0.0 μM	200	0.225	7.17	0.039	2.0	0.264	0.222	7.25	0.041	2.1
0.0 μM	0	0.213	6.84	0.025	2.1	0.238	0.214	6.80	0.022	2.1
20 μM	0	0.220	8.27	0.035	2.0	0.255	0.219	8.31	0.036	2.1
200 μM	0	0.235	7.84	0.019	~1.1[c]	0.254	0.231	7.95	0.015	2.1
2 mM	0	0.257	9.49	0.0026	~1.6[c]	0.260	0.256	9.50	0.0026	2.1
20 mM	0	0.265	9.91			0.265	0.265	9.93	0.0006	2.1
20 mM	200	0.254	9.75			0.254	0.252	9.83	0.0037	2.1

[a] Data were analyzed as a sum of exponentials. β_i and ϕ_i are the amplitudes and correlation times in nanoseconds, respectively. [b] Filtered indicates that a Cheng–Eisenfeld filter has been applied to the analysis, effectively fixing the lifetime of the short component of the fluorescence at 2.1 ns. [c] Indicates that the analysis for this lifetime did not satisfy the λ invariance criteria.

little apparent fast depolarization below approximately 1 ns. Therefore, under these conditions, we have a rigidly bound probe, as one would expect for dityrosine linked at each end to the polypeptide backbone of calmodulin. The anisotropy of the 0.0 mM calcium sample decays off faster and is not monoexponential.

The anisotropy data from the five calcium concentrations were analyzed by using the method of moments with λ invariance (Small & Isenberg, 1982). The calculated curves for the analyses of the data of Figure 3A are superimposed on the data, and the residuals are shown in Figure 3B,C. For the 20 mM calcium sample, we recover a cleanly resolved single correlation time of 9.9 ns (reduced $\chi^2 = 0.955$). Because of the stringent requirements of this kind of analysis, it is often possible to detect lack of resolution in decays before one can actually determine the values of the resolved decays. The analysis gave no hint of lack of resolution; λ invariance plots are flat, and lifetimes obtained by using different values of MD agree very closely. Repetition of the measurement gave an identical result. The anisotropy decay of the cross-linked calmodulin in the absence of calcium is not strictly monoexponential but analyzes as a sum of two exponentials with correlation times of 6.8 ns and about 2.1 ns. λ invariance plots indicate uncertainty in the recovered higher correlation time (values vary ±0.2 ns) and a considerable uncertainty in the shorter decay. The fits to the data for this and other low calcium measurements were not quite as good ($\chi^2 = 1.056$ for zero calcium); however, the data are not of sufficient quality to further resolve the decays.

The results for all five concentrations of calcium ion are summarized in Table I. Three different forms of the cross-linked calmodulin appear to exist—zero-, low-, and high-calcium forms with correlation times of about 7, 8, and 10 ns, respectively. The zero- and low-calcium forms are both biexponential, whereas the high-calcium form gives rise to a monoexponential decay.

The data in the absence of calcium were obtained in a solution containing 50 mM MOPS buffer and 10 μM EDTA at pH 7.5. Since circular dichroism (Hennessey et al., 1987) showed that potassium chloride folds calmodulin to essentially the same secondary structure as calcium, we wanted to see if the anisotropy change observed on the addition of calcium could be obtained by adding potassium chloride to the EDTA-containing solution. The results (Table I) show that potassium chloride does *not* induce the same change as calcium. With 200 mM KCl in the absence of calcium, the cross-linked calmodulin molecule remains in the zero-calcium form. At 200 mM KCl and 20 mM Ca²⁺, it is in the high-calcium form.

If the fluorescence anisotropy of the cross-linked calmodulin at high calcium concentration reflects simple rotational diffusion, then the recovered decay time should be directly pro-
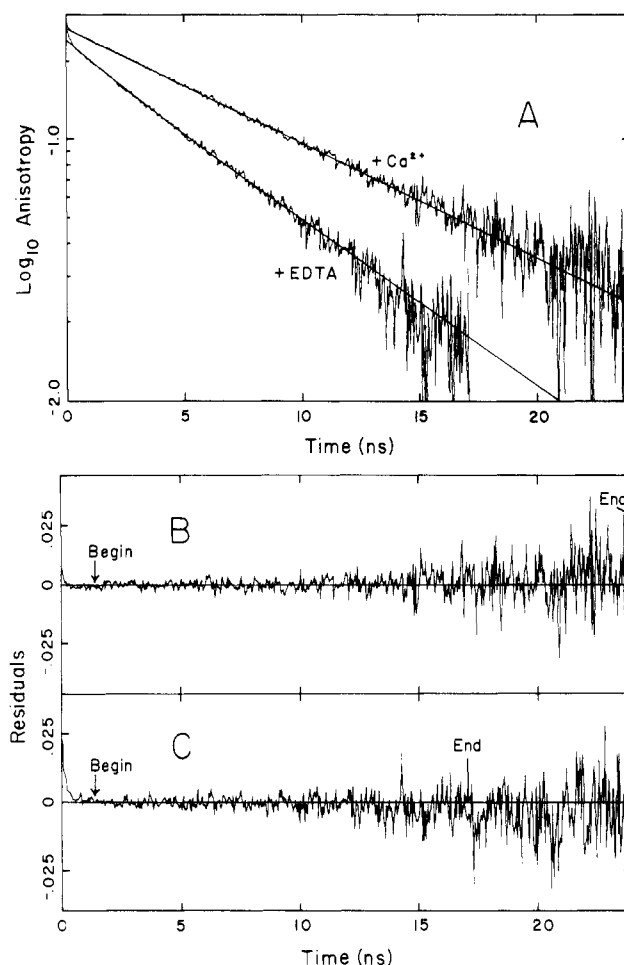

FIGURE 3: (A) Anisotropy decays of 1 μM cross-linked calmodulin in 0.0 and 20 mM calcium ion. Analysis was performed by using the method of moments as described in the text, and calculated curves are superimposed on the data. (B) and (C) are the residuals for the high and low calcium ion concentrations, respectively.

portional to the viscosity, η, and inversely proportional to the absolute temperature, T. A straightforward means of checking this is to measure the anisotropy as a function of temperature. The anisotropy decays of cross-linked calmodulin at high calcium ion concentrations were measured at seven different temperatures ranging from 4.8 to 31.8 °C. All of the analyses indicated monoexponential decays as in Figure 3. A plot of the inverse of the recovered correlation times vs. η/T is shown in Figure 4. The observed linear dependence strongly suggests that the measured decays represent rotational correlation times for the molecule. The straight line passes through zero because rotational diffusion must cease at 0 K or infinite viscosity. This plot also indicates that there are no conformational changes in the cross-linked calmodulin molecule which significantly

Table II: Analysis of Fluorescence Intensity Decays of Cross-Linked Calmodulin as a Function of Calcium Ion Concentration[a]

[Ca²⁺]	lifetimes (ns)				% of fluorescence[b]				τ_{av}[c]
	τ_1	τ_2	τ_3	τ_4	1	2	3	4	
0.0 μM	0.9	2.4	4.3	8.8	3.3	11.7	80.0	5.0	3.59
20 μM	0.5	1.8	4.2	7.6	1.5	7.9	82.8	7.8	3.56
60 μM	0.7	2.2	4.4	8.6	2.5	10.7	81.9	4.9	3.64
200 μM	0.5	1.9	4.4	9.4	1.3	10.0	84.6	4.1	3.63
600 μM	0.6	2.0	4.4	8.4	1.5	9.6	83.5	5.4	3.73
2.0 mM	0.7	2.2	4.5	9.3	1.6	11.7	83.5	3.2	3.78
6.0 mM	0.7	2.1	4.4	7.6	1.6	8.4	82.6	7.5	3.79
20 mM	0.4	1.3	4.0	6.3	0.4	4.6	73.8	21.3	3.81

[a] Cross-linked calmodulin concentration of 1 μM in 50 mM MOPS, pH 7.5. [b] Percent of fluorescence is calculated from 100 $(\alpha_i \tau_i / \sum \alpha_i \tau_i)$. [c] The weighted average lifetime, $\tau_{av} = \sum \alpha_i \tau_i / \sum \alpha_i$.
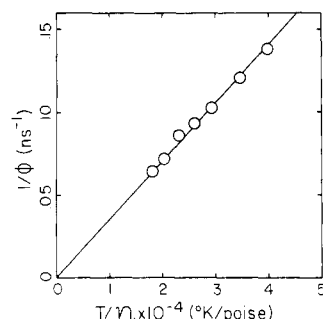

FIGURE 4: Reciprocal of the recovered anisotropy lifetimes for cross-linked calmodulin at high calcium concentration plotted as a function of η/T.

affects its rotational diffusion in the temperature range of 5–30 °C. (A less likely explanation is that conformational changes coincidentally mask what would otherwise be nonlinear behavior.)

The 2.1-ns correlation time recovered from the cross-linked calmodulin in the absence of calcium is too short to result from rotational diffusion and therefore must result from segmental flexibility of the molecule. As the calcium ion concentration is raised, it becomes increasingly difficult to resolve this short component. In order to get a better comparative measure of how much segmental flexibility is represented in the various decays, a Cheng–Eisenfeld filter was used to fix the value of the short correlation time to be 2.1 ns, and the analyses were repeated. The results are shown in Table I. The recovered amplitude, β_2, gives a qualitative estimate of how much short component can be recovered from the decays. In the absence of calcium and at low calcium concentrations, significant flexibility is observed. However, essentially none is observed at the highest calcium concentration.

Decay of the Fluorescence Intensity as a Function of Calcium Ion Concentration. Since the anisotropy of the fluorescence of the cross-linked calmodulin has a single-exponential form, it might be expected that the fluorescence intensity decay is also monoexponential. This turns out not to be true. Intensity decays (with the emission polarizer at the "magic angle") were measured at eight calcium ion concentrations from 0.0 to 20 mM. Each fluorescence decay curve contained about 2.4 × 10⁷ counts of data to reduce statistical errors and permit complex analyses. The data were deconvoluted and analyzed, with the results interpreted using λ invariance. All of the analyses recovered essentially the same four components, with a dominant lifetime of a little over 4 ns representing about 80% of the total fluorescence. This means that if the decay is a simple sum of exponentials, then it must be a sum of at least four components. The results of all eight analyses as a function of calcium ion concentration are listed in Table II along with the weighted average lifetime of the fluorescence.
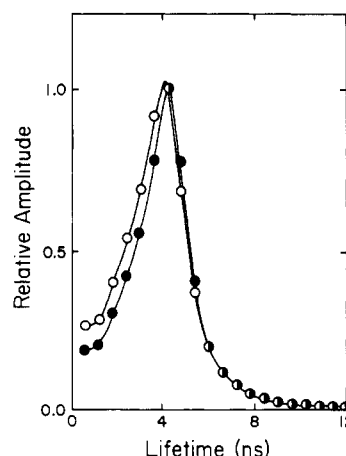

FIGURE 5: Distribution analyses of the fluorescence intensity decays of cross-linked calmodulin at 0.0 and 20 mM calcium.

A chromophore such as dityrosine, with two interacting ring systems, might in itself give rise to a heterogeneous fluorescence. To check for this possibility, we also examined the fluorescence decay of dityrosine (in 5.0 mM MOPS buffer at pH 7.0). Except for the presence of an apparent 3% impurity fluorescence with a shorter lifetime, dityrosine has a single-exponential lifetime of 4.30 ns.

Alcala et al. (1987) recently suggested that a smooth distribution of lifetimes, rather than a discrete sum, is a more suitable model for the intensity decay of chromophores bound to macromolecules. We have found, using synthetic data, that a Cheng–Eisenfeld filter can be used to recover the shape of such a distribution. Simply stated, by varying the fixed lifetime and performing a three- or four-component analysis, the recovered filtered amplitude provides a measure of the amount of decay present at a particular lifetime. We have no way of determining at this time whether it is more appropriate to analyze these data for a sum of exponentials or a distribution function. We believe that it will never be possible to distinguish the two models from data analysis alone. Results of distribution function analyses are included here, since they illustrate well the similarities between the intensity decays obtained in the presence and absence of Ca²⁺.

Distribution functions are shown in Figure 5 for cross-linked calmodulin at zero and 20 mM calcium. As the calcium concentration is increased, the distribution shifts slightly to higher lifetime and narrows slightly. Fewer short-lifetime components appear to be present. While these changes probably indicate a somewhat more homogeneous environment for the chromophore at higher calcium concentration, what is most remarkable about these plots is their close similarity.

On increasing the calcium ion concentration from 0.0 to 20 mM, the steady-state fluorescence intensity increases by a factor of 3.5. The change in intensity was also apparent when
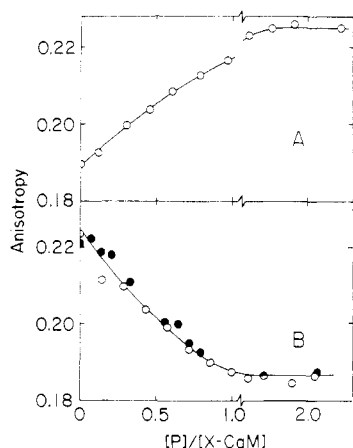
FIGURE 6: (A) Titration of a 1.0 μM solution of cross-linked cal-modulin with varying concentrations of troponin I. Conditions were 50 mM MOPS and 10 mM calcium acetate at pH 7.5 and 25.0 °C. Fluorescence excitation of the dityrosine fluorophore was at 320 nm with a 2-nm band-pass, and emission was measured through a Schott KV 380 cutoff filter. (B) Back-titration of the troponin I cross-linked calmodulin complex with varying concentrations of mastoparan (closed circles) and melittin (open circles). Conditions were 1.0 μM cross-linked calmodulin and either 3.0 μM (closed circles) or 2.4 μM (open circles) troponin I. Other conditions were the same as in (A). [P] is the molar concentration of the varied ligand (troponin I, mastoparan, or melittin), and [X-CaM] is the molar concentration of cross-linked calmodulin.

we measured the decays. However, neither the lifetimes nor their relative proportions of the decays change significantly. (The average lifetime of the fluorescence shown in Table II increases by only about 0.2 ns on the addition of calcium.) The large change in fluorescence intensity is apparently due to a change in static quenching. This interpretation agrees with the conclusion of Malencik and Anderson (1987), who showed that fluorescence intensity changes result from a shift in the pK_a value of the dityrosine as a function of calcium binding by the protein.

Binding of the Cross-Linked Calmodulin to Troponin I and to the Peptides Melittin and Mastoparan. Before performing anisotropy decay studies on complexes, we conducted steady-state measurements to verify that the proteins and peptides concerned associate with cross-linked calmodulin. Figure 6A shows the increase in steady-state anisotropy occurring when cross-linked calmodulin is titrated with rabbit skeletal muscle troponin I (Tn I), a widely used model cal-modulin-binding protein of molecular weight 21 000. The end point of the titration shows the binding of 1.1 mol of Tn I per mole of cross-linked calmodulin. Mastoparan (Malencik & Anderson, 1983) and melittin (Barnette et al., 1983; Comte et al., 1983; Malencik & Anderson, 1984) are amphipathic basic polypeptides—containing 14 and 26 amino acid residues, respectively—which are avidly bound by native calmodulin. Back-titration of the cross-linked calmodulin–Tn I complex with these peptides confirms the complete displacement of Tn I upon the addition of either 1 mol of mastoparan or 1 mol of melittin (Figure 6B). The ability of stoichiometric quantities of mastoparan to displace Tn I was previously shown for un-modified calmodulin (Anderson & Malencik, 1986).

Anisotropy decays were measured for the complexes between the cross-linked calmodulin and mastoparan, melittin, and troponin I, and the analysis results are shown in Table III.

DISCUSSION

Heterogeneous Fluorescence of the Cross-Linked Calmo-dulin. Although dityrosine itself has a monoexponential fluorescence decay with a lifetime of 4.30 ns, the fluorescence

Table III: Analyses of Anisotropy Decays of Cross-Linked Calmodulin Bound to Troponin I and Peptides[a]

addition	β_1	ϕ_1	β_2	ϕ_2	χ^2
none	0.265	9.9			0.955
mastoparan	0.256	11.9	0.017	2.3	1.083
melittin	0.257	11.2			1.034
troponin I	0.233	22.1	0.012	3.5	1.074

[a] Data were analyzed as a sum of exponentials. β_i are the recovered amplitudes and ϕ_i the recovered correlation times in nanoseconds. χ^2 is defined under Materials and Methods.

of the cross-linked calmodulin is not as homogeneous. A source of the heterogeneity could be the presence of more than one photoproduct in solution. However, the excitation and emission spectra of neutralized acid hydrolysates are identical with those of dityrosine. By using a 310-nm narrow bandwidth excitation source, only dityrosine-containing protein should contribute to the fluorescence. Perhaps some of the molecules are locked in different configurations. The monoexponential anisotropy decays from the high-calcium form, however, would argue against the presence of cross-linked protein molecules which differ significantly from one another in structure. The hete-rogeneity of the fluorescence intensities is probably due to the chromophore simply finding slightly different environments within the protein. A single-exponential anisotropy could result if the overall conformational state of the cross-linked calmo-dulin is essentially the same for each state of the chromophore, and if interconversion between different states of the chro-mophore occurs either very fast or very slowly compared to the lifetime of the fluorescence.

Segmental Motion vs Rotational Diffusion. The X-ray crystallographic studies on the native calcium–calmodulin complex revealed a dumbbell-shaped molecule, with two lobes of approximate dimensions 25 × 20 × 20 Å. The lobes are separated by an eight-turn segment of α-helix, resulting in a total length of about 65 Å (Babu et al., 1985). Such a structure would appear to be inherently flexible. In fact, the tyrosine fluorescence anisotropy of unmodified calmodulin is dominated by short-lifetime segmental flexibility in both the low- and high-calcium states, with correlation times of 2.1 and 3.4 ns, respectively (unpublished results). However, the di-tyrosine anisotropy decay of the calcium-saturated derivative is monoexponential, showing no evidence of flexibility (see Figure 3A and Table I). The low-calcium form of cross-linked calmodulin, on the other hand, shows a small, significantly faster component in depolarization, with an apparent decay time of about 2.1 ns. The location and orientation of the dityrosine chromophore in the calcium-saturated derivative may be such that segmental flexibility does not cause signif-icant depolarization of the fluorescence. Another possibility is that the intramolecular cross-link between positions 99 and 138 reduces the flexibility of the calcium–calmodulin complex. Since the cross-linked calmodulin in the absence of calcium does show significant fast depolarization, we conclude either that the chromophore can now report on the flexibility or, more likely, that this state of the protein is significantly more flexible.

If we assume a simple model in which segmental motions of the dityrosine occur independently of rotational diffusion, then we can calculate the correlation time of the segmental motion. Let ϕ_s be the correlation time of this motion and ϕ_r be the rotational correlation time of the macromolecule. Under these conditions, the anisotropy is a product of the separate factors responsible for depolarization (Lakowicz, 1983):

$$r(t) = r_0[\alpha e^{-t/\phi_s} + (1 - \alpha)]e^{-t/\phi_r} \qquad (5)$$

The anisotropy should be a sum of two exponentials with rates

of $1/\phi_r$ and $1/\phi_r + 1/\phi_s$. r_0 is the limiting anisotropy, a function of the chromophore itself, and α is the fraction of the initial anisotropy decaying due to segmental motion. If we take 6.84 ns to be the rotational correlation time of the low-calcium form, then this conformation of the cross-linked calmodulin possesses segmental motion with a correlation time of 3.0 ns and α equals about 0.1. r_0 is related to the angle, θ, between the absorption and emission dipoles by the equation (Weber, 1966):

$$r_0 = (3 \cos^2 \theta - 1)/5 \qquad (6)$$

The value of 0.265 found for r_0 for the cross-linked calmodulin at high calcium concentration would result from a 28° angle between the absorption and emission transition moments.

It appears in Figure 5 that the fluorescence properties of the chromophore remain essentially unaffected by an increase in the calcium ion concentration. If eq 5 holds and there are no other depolarizing processes, then the sum of the amplitudes of the measured anisotropy, $\beta_1 + \beta_2$, should remain constant. We note from Table I, however, that the sum decreases slightly on decreasing calcium concentration with a distinctly lower value for the sample in the absence of calcium. We believe this decrease results from residual very fast depolarizing motions of the chromophore on a time scale not resolved by these measurements. (Strictly speaking, one should modify eq 5 to accommodate the small contribution of this additional component.) Note that KCl appears to increase the local rigidity of the chromophore.

Rotational Diffusion Calculations. In order to calculate rotational diffusion coefficients for different shapes, we must first estimate the molecular volume of the cross-linked calmodulin. The molecular weight is 16 700, and the partial specific volume, $\bar{v}$, is 0.707 cm³/g in the presence of calcium ion and 0.712 cm³/g in its absence (Crouch & Klee, 1980). Assuming a hydration of 0.20 cm³ of water/g of protein, we find a molecular volume of about 25 200 Å³. This degree of hydration is a value frequently used for rotational diffusion calculations (Lakowicz, 1983) and is only a guess. Its effect on the uncertainty of the calculations is discussed below.

The rotational correlation time for a sphere in a medium of viscosity η is given by the well-known expression:

$$\phi = \eta V/kT \qquad (7)$$

where k is Boltzmann's constant and T is the absolute temperature. Thus, if the cross-linked calmodulin were a perfect sphere, we should observe a correlation time of about 6.2 ns. Since in the absence of calcium we find a low value of 6.84 ns, we conclude that under these conditions the molecule is nearly spherical.

In order to compare the recovered correlation times to those expected for the native calmodulin molecule, we have calculated the rotational diffusion coefficient for the dumbbell-shaped structure demonstrated in the X-ray crystallographic studies. The hydrodynamic properties of the dumbbell were described by de la Torre and Bloomfield (1977a,b). Their model consists of two large spheres of diameter σ_1 separated by a chain of smaller spheres of diameter σ_2 and total length L. The original calculations of the properties of this model required the numerical solution of an extensive set of simultaneous hydrodynamic interaction equations. These calculations do not need to be repeated. To find the rotational diffusion coefficient for rotation of the dumbbell about an axis perpendicular to the main symmetry axis, the authors give a polynomial interpolation equation which approximates the solution [eq 45 and Table II in de la Torre and Bloomfield (1977b)]. This is the equation that we use here, and we call

this diffusion coefficient D_2. de la Torre and Bloomfield (1977b) specify that the range of validity of the polynomial coefficients is $L/\sigma_1 \leqslant 16$ and $\sigma_1/\sigma_2 \geqslant 1$, where the approximation reproduces the original values within ±6%. The parameters used here are well within the specified ranges. The polynomial approximation, of course, automatically permits interpolation for nonintegral numbers of small spheres connecting the lobes.

For our anisotropy calculations, we also require D_1, the rotational diffusion coefficient for rotation about the main symmetry axis. First we assume that the frictional coefficient for rotation about the main axis, C_{sum}, is equal to the sum of the frictional coefficients of the spheres of the model. D_1 is inversely proportional to the total frictional coefficient for rotation about the axis (Weber, 1953; Memming, 1961):

$$D_1 = kT/C_{sum} \qquad (8)$$

where k is Boltzmann's constant and T is the absolute temperature. Since the rotational friction coefficient, C_0, for a sphere is equal to

$$C_0 = 8\pi\eta\sigma^3 \qquad (9)$$

where η is the viscosity:

$$D_1 = \frac{kT}{4\pi\eta} \frac{1}{4\sigma_1^3 + L\sigma_2^2} \qquad (10)$$

The fluorescence anisotropy decay for a general-shaped rigid body undergoing Brownian rotation is a sum of a maximum of five exponentials (Belford et al., 1972; Chuang & Eisenthal, 1972; Ehrenberg & Rigler, 1972). To find the functional form of the anisotropy for a cylindrically symmetric shape such as a dumbbell, one sets two of the rotational diffusion coefficients equal. The five exponentials simplify to three:

$$r(t) = \gamma_1 e^{-(4D_1 + 2D_2)t} + \gamma_2 e^{-(D_1 + 5D_2)t} + \gamma_3 e^{-(6D_2)t} \qquad (11)$$

where

$$\gamma_1 = (6/5)\alpha_2\epsilon_2\alpha_3\epsilon_3 + (3/10)(\alpha_2^2 - \alpha_3^2)(\epsilon_2^2 - \epsilon_3^2)$$

$$\gamma_2 = (6/5)\alpha_1\epsilon_1(\alpha_2\epsilon_2 + \alpha_3\epsilon_3)$$

$$\gamma_3 = (3/5)\alpha_1^2\epsilon_1^2 + (3/10)(1 - \alpha_1^2)(1 - \epsilon_1^2) - (1/5)$$

α_i and ϵ_i are the direction cosines of the angles formed by the absorption and emission dipoles with respect to a set of molecular axes. A subscript of 1 refers to angles formed with the symmetry axis, and subscripts of 2 and 3 refer to angles formed with a set of axes in a plane perpendicular to the symmetry axis. (Ordinarily, these amplitudes are simplified further since the directions of two of the axes can be considered arbitrary, but we have retained this form for calculations presented below.)

The three rotational correlation times expected for a dumbbell with a volume of 25 200 Å³ were calculated assuming $\sigma_2 = 3.5$ Å [results are quite insensitive to the value of σ_2 (de la Torre & Bloomfield, 1977b)]. Plots of these lifetimes are shown in Figure 7 as a function of the total length ($=L + 4\sigma_1$). The measured value of 9.9 ns for the protein at high calcium concentration must be one of the two higher lifetimes or an unresolved mixture of them. Choosing one or the other places a range of possible values of the length of the structure of between about 62 and 66 Å. Such a length could be regarded as somewhat short for the fully hydrated X-ray crystallographic structure but still basically consistent with it. In Figure 8, the 64-Å dumbbell shape used for one set of calculations in Figure 7 is shown approximately to scale superimposed on a tracing of the X-ray crystallographic structure (Babu et al., 1985).
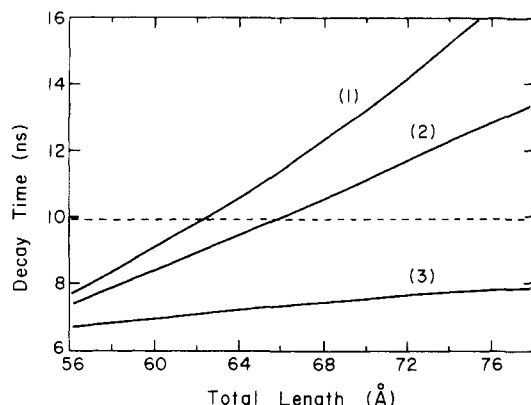
FIGURE 7: Three rotational correlation times expected for the dumbbell model shown in Figure 8 as a function of total length $(L + 4\sigma_1)$. For these calculations, $\sigma_2 = 3.5$. Since the volume is held constant at 25 200 Å^3, σ_1 is approximately 14 Å and decreases slightly on increasing total length. A horizontal line is drawn at 9.9 ns, the measured rotational correlation time for the cross-linked calmodulin at high calcium ion concentration.
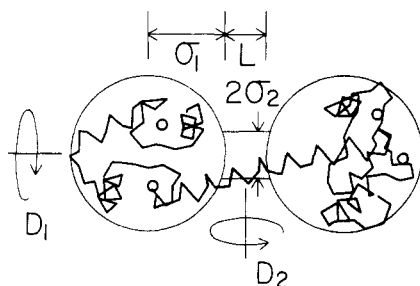

FIGURE 8: Tracing of the X-ray crystallographic structure of the calcium-bound calmodulin from Babu et al. (1985), superimposed approximately to scale on the 64-Å dumbbell shape used for the rotational diffusion calculations.

Not knowing which lifetime to choose is a major source of uncertainty in these hydrodynamic calculations. Another is the lack of a good measure of the hydration for rotational diffusion. Doubling the hydration from 0.2 to 0.4 decreases the predicted length of the structure to a range of 61–63 Å, not a large change, but the corresponding increase in volume requires that the lobes of the dumbbell nearly touch. It seems reasonable, however, to expect hydration to be greatest near the center of the structure where bound water molecules would experience the least displacement force resulting from rotary motion.

If the anisotropy for the rotational diffusion of the dumbbell is a sum of three exponentials, then why do we observe only a single decay for the high-calcium form? Since we estimated the average angle between the absorption and emission dipoles to be 28°, we can calculate amplitudes that would correspond to different alignments of the chromophore with the molecular axes. We show an example of such a set of calculations in Figure 9. For this particular plot, the absorption dipole, the emission dipole, and the symmetry axis of the molecule remain in the same plane. ψ is defined as the angle between the absorption dipole and the symmetry axis. At the left-hand side of the plot, we begin with ψ equal to -20°. Since the angle between the dipoles is 28°, the emission dipole begins at 8°. The plot ends at the point where the absorption dipole has reached the plane perpendicular to the symmetry axis and the emission dipole is 28° below the plane.

We note from eq 11 that the absorption and emission dipoles are interchangeable. Note also that at any value of ψ all three amplitudes sum to r_0 (0.265). If either dipole aligns with the main symmetry axis or is perpendicular to it, the amplitude

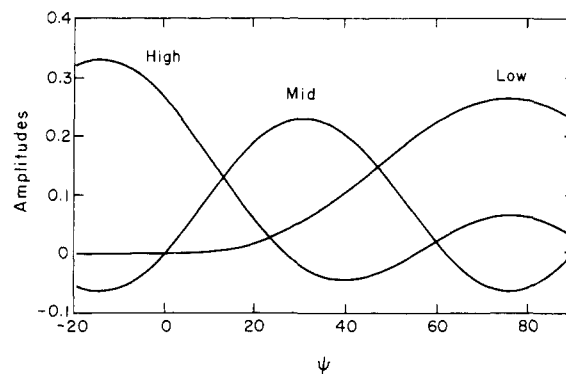
FIGURE 9: Anisotropy decay amplitudes calculated for the dumbbell model of Figure 7 according to eq 9. Amplitudes corresponding to the high (H), middle (M), and low (L) lifetimes are labeled on the plot. The angle between the absorption and emission dipoles (8 in eq 4) is assumed to be 28°. The angle ψ, which rotates the dipoles, is defined in the text.

of the middle lifetime becomes zero. These features can be easily observed in Figure 9.

We would be unable to resolve the two higher lifetimes such as the 10.4- and 9.4-ns decays found in Figure 9 for the 64-Å dumbbell shape. At almost any angle shown in the figure, we would expect to recover only a single lifetime. For example, if both dipoles are on opposite sides of the symmetry axis at angles of -14° and 14°, then 10.4 ns would not be resolved from a small negative component of lifetime 9.4 ns. If both dipoles are nearly perpendicular to the axis, then the small positive and negative contributions from the long and middle lifetimes would nearly cancel, and one would measure only the short decay. There are only a few possible orientations between about 50° and 60° where one would expect to measure decays which would be clearly more complex than a single exponential. We would conclude from this plot of amplitudes that the 9.9-ns decay that we measure for the high-calcium form results from the long lifetime or an unresolved mixture of the long and middle lifetimes. It is straightforward to show using plots such as Figure 9 or algebraic approximations of eq 11 that similar conclusions can be drawn for other relative orientations of the dipoles.

Model of the Observed Conformational Changes. The X-ray crystallographic structure (Babu et al., 1985) for the native calcium-bound form of calmodulin shows each lobe of the dumbbell to contain three short segments of α-helix. The two lobes are connected by an eight-turn α-helix. Two calcium-binding sites are found on each lobe of the dumbbell—binding sites I and II at the N-terminal end of the protein and sites III and IV at the C-terminal end. Each site is composed of a helix–loop–helix binding domain. Since sites II and III involve the central α-helix as part of the binding domain, Babu et al. (1985) suggest that the action of calcium ion binding might be to extend the calmodulin molecule at this juncture. Removing the calcium ions from these two sites would permit the collapse of the structure to a more compact form. This model is consistent with our results. It is also consistent with the circular dichroism results which show only very small changes in the secondary structure on the binding of calcium ions in the presence of 200 mM KCl (Hennessey et al., 1987).

Our anisotropy results indicate a highly compact but flexible structure for the cross-linked calmodulin in the absence of calcium. At low calcium concentrations (20–200 μM), we find an intermediate length structure. At high calcium concentrations (2–20 mM), we find an elongated structure which is close to, or the same as, the extended dumbbell structure observed by X-ray crystallography for the native high-calcium

Table IV: Rotational Correlation Times Predicted for Complexes on the Basis of Volume Increases[a]

complex	mol wt	$\bar{v}$	V	$V_{complex}$	ϕ_{pred}	ϕ_{meas}
X-CaM	16700	0.707	25200			9.9
mastoparan	1479	0.805	2469	27700	10.9	11.9
melittin	2829	0.770	4558	29700	11.7	11.2
troponin I	21000	0.719	32000	57200	22.5	22.1

[a] Molecular weights and partial specific volumes, $\bar{v}$ in cubic centimeters per gram, of mastoparan and melittin were calculated from amino acid sequences. Values for troponin I are from Grand and Wilkinson (1977). V is the volume in Å^3 of the complex calculated by assuming a hydration of 0.2 cm^3 of water/g of protein. ϕ_{pred} is the rotational correlation time in nanoseconds predicted for the complex assuming that the rotational correlation times are simply proportional to the volume. ϕ_{meas} is the observed rotational correlation time from Table III.

form. In native calmodulin, calcium-binding sites I and II at the N-terminal end of the protein are believed to have a lower affinity for calcium ions than sites III and IV [cf. review by Forsén et al. (1986)]. However, the relative affinities of these pairs of sites may be reversed in the cross-linked calmodulin (Malencik & Anderson, 1987). If the calcium-binding sites at one end of the molecule fill first, then the protein will be elongated to an intermediate length. The subsequent occupation of the other pair of sites would then fully extend the molecule.

Binding of Melittin, Mastoparan, and Troponin I. From Figure 6 and Table III, we see that mastoparan, melittin, and troponin I each bind strongly to the cross-linked calmodulin such that the complexes each rotate as a unit. The anisotropy from the melittin complex remains monoexponential in character, but the anisotropy of the mastoparan and troponin I complexes begins to show a small amount of segmental flexibility. Although the data from the mastoparan and troponin I complexes analyze as double exponentials, each of the analyses has only a single decay of magnitude sufficient to be a rotational correlation time. A simple calculation was made to see if binding results in a major change in conformation. The results are shown in Table IV. The table compares the observed rotational correlation times for the complexes with the values that would be expected if the increases in correlation times were simply proportional to the changes in volume resulting from binding.

From Table IV, we observe that the binding of neither mastoparan nor melittin results in a *major* structural change. However, the two peptides show different properties. The correlation time of the mastoparan complex is longer than that which would be predicted from volume changes alone. Either the binding of mastoparan results in elongation of the calmodulin molecule or the bound peptide extends sufficiently outward from calmodulin to increase the rotational correlation time. Melittin, on the other hand, may bind near the center of the molecule or decrease the extension of the structure somewhat.

CONCLUSIONS

This paper explores the use of dityrosine as a fluorophore for examining the rotational diffusion of calmodulin and complexes formed between calmodulin and other peptides and proteins. The fortuitous discovery of dityrosine formation in calmodulin (Malencik & Anderson, 1987) has led to the present work which shows its use for studying calmodulin structure and function. Linkage of tyrosines-99 and -138 to form dityrosine results in a rigid chromophore tethered to the protein backbone. This linkage means that fluorescence anisotropy studies on cross-linked calmodulin can report on ro-

tational diffusion of the entire protein rather than predominantly local segmental flexibility as would be reported by monomeric tyrosine residues. The dynamic fluorescence anisotropy measurements described here are consistent with a dumbbell shape for cross-linked calmodulin at high calcium ion concentration, and a compact shape in the absence of calcium. The large shape changes reported here as a function of calcium ion concentration are consistent with those reported for non-cross-linked calmodulin using small-angle X-ray scattering (Seaton et al., 1985), although the present measurements appear to indicate a somewhat more compact structure in the absence of calcium.

REFERENCES

Alcala, J. R., Gratton, E., & Prendergast, F. G. (1987) *Biophys. J. 51*, 597.

Amado, R., Aeschbach, R., & Neukom, H. (1984) *Methods Enzymol. 107*, 377.

Anderson, S. R., & Malencik, D. A. (1986) *Calcium Cell Funct. 6*, 1.

Anderson, S. R., & Malencik, D. A. (1987) in *Fluorescent Biomolecules: Methodologies and Applications* (Jameson, D., Ed.) Plenum Press, New York (in press).

Babu, Y. S., Sack, J. S., Greenhough, T. J., Bugg, C. E., Means, A. R., & Cook, W. J. (1985) *Nature (London) 315*, 37.

Badea, M. G., & Brand, L. (1979) *Methods Enzymol. 61*, 378.

Barnette, M. S., Daly, R., & Weiss, B. (1983) *Biochem. Pharmacol. 19*, 387.

Belford, G. G., Belford, R. L., & Weber, G. (1972) *Proc. Natl. Acad. Sci. U.S.A. 69*, 1392.

Brostrom, C. O., Huang, Y. C., Breckenridge, B. McL., & Wolff, D. J. (1975) *Proc. Natl. Acad. Sci. U.S.A. 72*, 64.

Cheng, S. W., & Eisenfeld, J. (1979) in *Applied Nonlinear Analysis* (Lakshmikantham, B., Ed.) p 485, Academic Press, New York.

Cheung, W. Y. (1967) *Biochem. Biophys. Res. Commun. 29*, 478.

Cheung, W. Y., Bradham, L. S., Lynch, T. J., Lin, Y. M., & Tallant, E. A. (1975) *Biochem. Biophys. Res. Commun. 66*, 1055.

Chuang, T. J., & Eisenthal, K. B. (1972) *J. Chem. Phys. 57*, 5094.

Comte, M., Maulet, Y., & Cox, J. A. (1983) *Biochem. J. 209*, 269.

Crouch, T. H., & Klee, C. B. (1980) *Biochemistry 19*, 3692.

de la Torre, J. G., & Bloomfield, V. A. (1977a) *Biopolymers 16*, 1747.

de la Torre, J. G., & Bloomfield, V. A. (1977b) *Biopolymers 16*, 1765.

Ehrenberg, M., & Rigler, R. (1972) *Chem. Phys. Lett. 14*, 539.

Forsén, S., Vogel, H. J., & Drakenburg, T. (1986) *Calcium Cell Funct. 6*, 114.

Grand, R. J. A., & Wilkinson, J. M. (1977) *Biochem. J. 167*, 183.

Hennessey, J. P., Jr., Manavalan, P., Johnson, W. C., Jr., Malencik, D. A., Anderson, S. R., Schimerlik, M. I., & Shalitin, Y. (1987) *Biopolymers 26*, 561.

Isenberg, I., & Small, E. W. (1982) *J. Chem. Phys. 77*, 2799.

Kilhoffer, M.-C., Demaille, J. G., & Gerard, D. (1981) *Biochemistry 20*, 4407.

Klee, C. B. (1977) *Biochemistry 16*, 1017.

Lakowicz, J. R. (1983) in *Principles of Fluorescence Spectroscopy*, p 161, Plenum Press, New York.

Lambooy, P. K., Steiner, R. F., & Sternberg, H. (1982) *Arch. Biochem. Biophys. 217*, 517.

Libertini, L. J., & Small, E. W. (1982) *Rev. Sci. Instrum. 54*, 1458.

Libertini, L. J., & Small, E. W. (1987) *Anal. Biochem. 163*, 500.

Malencik, D. A., & Anderson, S. R. (1983) *Biochem. Biophys. Res. Commun. 114*, 50.

Malencik, D. A., & Anderson, S. R. (1984) *Biochemistry 23*, 2420.

Malencik, D. A., & Anderson, S. R. (1987) *Biochemistry 26*, 695.

Memming, R. (1961) *Z. Phys. Chem. (Leipzig) 28*, 168.

Perry, S. V., Cole, H. A., Hudlicka, O., Patchell, V. B., & Westwood, S. A. (1984) *Fed. Proc., Fed. Am. Soc. Exp. Biol. 43*, 3015.

Potter, J. D. (1982) *Methods Enzymol. 85*, 241.

Seamon, K. B. (1980) *Biochemistry 19*, 207.

Seaton, B. A., Head, J. F., Engelman, D. M., & Richards, F. M. (1985) *Biochemistry 24*, 6740.

Small, E. W., Libertini, L. J., & Isenberg, I. (1984) *Rev. Sci. Instrum. 55*, 879.

Weber, G. (1953) *Adv. Protein Chem. 8*, 415.

Weber, G. (1966) in *Fluorescence and Phosphorescence Analysis* (Hercules, D., Ed.) p 217, Interscience, New York.

Wolff, D. J., Poirier, P. G., Brostrom, C. O., & Brostrom, M. A. (1977) *J. Biol. Chem. 252*, 4108.

^{2}H Nuclear Magnetic Resonance of Exchange-Labeled Gramicidin in an Oriented Lyotropic Nematic Phase[†]

James H. Davis

Guelph-Waterloo Program for Graduate Work in Physics, Department of Physics, University of Guelph, Guelph, Ontario, Canada N1G 2W1

Received July 30, 1987

ABSTRACT: Lyotropic nematic liquid-crystalline phases, such as that formed by potassium laurate/decanol/KCl/water, are found to accept readily large amphiphilic solute molecules. Since these phases spontaneously orient in high magnetic fields, it becomes possible to obtain NMR spectra of biologically interesting solutes in an oriented axially symmetric environment. The amide hydrogens of the peptide backbone of gramicidin D (Dubos) were exchanged for deuterium, and the gramicidin was incorporated into a lyotropic nematic phase made with deuteriated buffer in place of water. ^{2}H NMR spectra of oriented, exchange-labeled gramicidin were then obtained. The strong water signal from the deuteriated buffer was eliminated by using selective excitation and a polynomial subtraction procedure. The ^{2}H NMR spectra at high temperature consist of twelve major quadrupolar doublets. The splittings observed are largely independent of temperature, suggesting a highly rigid backbone structure. Two of the doublets, which are chemically shifted relative to the others, show stronger temperature dependence. These two probably arise from the exchangeable amino hydrogens on the tryptophan indole moieties of the peptide. While we cannot yet assign all of the doublets, the spectra and nuclear magnetic relaxation data are consistent with a rigid slightly distorted $\beta_{LD}^{6.3}$ helix undergoing axially symmetric reorientation about the director of the liquid-crystalline phase. The correlation time for the axially symmetric reorientation is determined by relaxation measurements to be about 10^{-7} s.

The natural pentadecapeptides, gramicidins A, B, and C, from *Bacillus brevis* are fascinating analogues of integral membrane proteins (the natural mixture is referred to as gramicidin D and contains approximately 85% gramicidin A, and the remainder consists of gramicidins B and C which differ only in the substitution of Trp[11] with phenylalanine or tyrosine). Mixed with phospholipids, such as 1,2-dimyristoyl-*sn*-glycero-3-phosphocholine (DMPC),[1] and water, two molecules of gramicidin form a transbilayer channel capable of con-

ducting an ionic current (e.g., of Na or K ions) across the bilayer (Hladky & Haydon, 1972; Barrett Russell et al., 1986; Anderson, 1983). The structure of this transmembrane channel has been the subject of much study and some controversy (Urry et al., 1983; Urry, 1985; Weinstein et al., 1980; Wallace, 1983; Arseniev et al., 1985). The best model for the channel structure, at present, is that of a head-to-head di-

[1] Abbreviations: DMPC, 1,2-dimyristoyl-*sn*-glycero-3-phosphocholine; DPPC, 1,2-dipalmitoyl-*sn*-glycero-3-phosphocholine; TMS, tetramethylsilane; DANTE, delays alternating with nutations for tailored excitation.